Experimental Investigation on the Design of Nozzle/Diffuser for Micropumps

Shun-Fa Hwang[1], Ying-Min Ji[1]
[1]Department of Mechanical Engineering, National Yunlin University of Science and Technology, Yunlin

Abstract

To design a planar nozzle/diffuser, its two parameters, divergence angle and slenderness, are investigated in this work under experimental evaluation of the flow rate of the assembled micropump. Thirteen micropumps with different design of nozzle/diffuser are chosen from the no stall region, transitory region, and bistable steady stall region in a complete stability map of diffuser flow patterns. These micropumps actuated by piezoelectric buzzer are fabricated by UV photolithography. The measured results indicate that those micropumps having better performance are located in the transitory region where the flow is strongly unsteady. The best two nozzles/diffusers occur at the line of the maximum pressure recovery.

Keywords: Micropump, Nozzle/Diffuser, Piezoelectric Buzzer, Divergence Angle, Slenderness

1. Introduction

Because of the fast development in microelectromechanical system (MEMS) technologies, micropumps, one of the key components in a microfluid system, have been received much attention since 1980. The main function of micropumps is to deliver precise amount of fluid from one place to another place. Micropumps have extensive applications including lab-on-a chip, embedded medical devices, and printer heads. Generally, micropumps, especially mechanical ones, consist of two main parts, actuating chamber and inlet/outlet. Actuating chamber is a chamber with an actuated diaphragm which has oscillatory motion. Different actuation methods such as piezoelectric, electrostatic, thermopneumatic, electromagnetic, and shape memory alloy have been proposed. Among these actuation methods, piezoelectric actuation has a large potential because of high pump performance, relatively simple structure, and no heat problem. One way of piezoelectric actuation is to glue a PZT disc on the top of a membrane with conductive epoxy, thus forming a unimorph actuator. Another way is to deposit the piezoelectric material directly onto the membrane. However, there is an adhesion problem between the attached PZT disc and the membrane, and the manufacturing process of direct deposition is complicated.

The inlet/outlet part is the gates of a micropump and could be further divided into two types. One type uses passive check valves [1] in which the cantilever membrane of inlet will open under supply mode while the cantilever membrane of outlet will open under pump mode. The other type uses valveless nozzle/diffuser elements [2]. A valveless micropump has a net transport of fluid from the inlet to the outlet due to the difference in the flow resistances in the diffuser and nozzle. Since passive check valves have the drawbacks of wear, clogging, and fatigue, nozzle/diffuser is popular in recent micropumps. According to the shape, they could be classified as conical, pyramidal, and planar. Among them, the planar nozzle/diffuser is commonly used.

To achieve the best performance of piezoelectrically actuated valveless micropumps, one possibility is to design the nozzle/diffuser element for the highest flow capability. Olsson et al. considered the pressure loss coefficient in the three regions of the nozzle/diffuser element with the assistance of the figure of flow losses in a gradual conical expansion region from the viewpoint of macroscopic internal flow [3]. Nozzle/diffuser elements with different lengths and divergence angles are considered. Olsson et al. used both numerical and experimental methods to study the flow-directing capability and the flow pattern for both the diffuser element and the nozzle element [4]. Yang et al. investigated the flow characteristics within a nozzle/diffuser finding that the pressure loss coefficient for a nozzle/diffuser decrease with the Reynolds number and the nozzle/diffuser length has little influence on the pressure loss coefficient [5]. Singhal et al. used commercial software to discuss the flow characteristics of low Reynolds number laminar flow through gradually expanding conical and planar diffusers [6]. Their results indicated that pressure loss coefficient at low Reynolds numbers vary significantly with Reynolds number and the trends of variation in the pressure loss coefficient with Reynolds number are different for small and large diffuser angles. Yao et al. numerically simulated three-dimensional transient flow in valveless micropumps and improved the flow rate by modifying the geometry of the diffusers [7]. Izzo et al. proposed a new diffuser with some properly shaped vortex area to improve its efficiency used in a micropump [8]. Wang et al. investigated the loss characteristics of flat-walled microdiffusers for Reynolds number between 100 and 2000 and found that the diffuser angle corresponding to the optimum diffuser efficiency varies from 40 at Reynolds number 100 to 20 for Reynolds number larger than 500 [9]. Chen et al. tested PDMS

micro-diffuser/nozzle and obtained that the pressure loss coefficients for both nozzle and diffuser decrease with the Reynolds number [10].

Since the nozzle/diffuser is just parts of a micropump, there are other factors such as inlet and outlet channels, chamber volume, actuation method, etc. that may affect the performance of a micropump. To focus on the effect of planar nozzle/diffuser, its two parameters, divergence angle and slenderness that is the ratio of diffuser length to entrance width, are investigated in this work under experimental evaluation of the flow rate of the assembled micropump. Ultra-violet (UV) photolithography that is also called UV-LIGA is adopted to fabricate the micropump, and an acid-catalyzed negative photoresistive material, SU8-50, is used as a structure material. A commercially available piezoelectric buzzer is used as actuation membrane under driving frequencies less than 300 Hz. From the experimental results, the possible best values of the divergence angle and slenderness are identified.

2. Specimens

The structure of a valveless micropump with piezoelectric buzzer is illustrated in Fig. 1. As shown, it is composed of four parts: PDMS (polydimethylesiloxane) cover, piezoelectric buzzer, SU-8 micro-structure, and silicon wafer. The cover fabricated from PDMS is used to provide the necessary cover over the micro-chamber without interfering the vibration of the buzzer. Piezoelectric buzzer is a brass disk glued with piezoceramic layer. The piezoelectric buzzer has 7 mm diameter of brass disk and 5 mm diameter of piezoceramic layer. This buzzer is commercially available and its thickness is only 0.12 mm. Since the piezoelectric buzzer is already a unimorph form, no other membrane is needed to attach to it. The micro-structure fabricated from SU-8 photoresist includes a cylindrical chamber, a diffuser, and a nozzle. The silicon wafer used in this work is just as a bottom layer such that the SU-8 micro-structure could grow on it.

From the design viewpoint, the most important part of a valveless micropump is the micro-structure. In this structure, the diameter of the cylindrical chamber should be compatible to the size of the chosen buzzer. Therefore, under the decided diameter and height of the micro-structure, the part to be designed is the nozzle/diffuser. As shown in Fig. 2, there are three parameters in a nozzle/diffuser. Since only two of them are independent, the divergence angle (2θ) and the slenderness (L/W_1) are considered in the design process. For a macro-diffuser, a complete stability map of diffuser flow patterns is shown in Fig. 3 with these two parameters [11]. As shown in this figure, there is a region called “no stall” below the line *aa*, in which there is steady viscous flow, no separation, and moderately good performance. There is a transitory steady stall region between lines *aa* and *bb* and the flow is strongly unsteady. The best performance occurs in this region. Between lines *bb* and *cc* there is a steady bistable stall region, where the stall pattern could flip-flop from one wall to the other and the performance is poor. In the jet flow region the flow separates completely from the walls making performance extremely poor. Even though the present diffusers are under the micro-range, the divergence angle and slenderness are still chosen to systematically design the diffuser. Thirteen diffusers with the dimensions listed in Table 1 are investigated. As shown in Fig. 3, these diffusers are distributed in three regions except for the jet flow region. Especially, there are 8 diffusers in the transitory steady stall region.

3. Fabrication process and experimental setup

The micro-structure was fabricated by employing UV exposure and film mask on SU-8 photoresist. The thickness of the micro-structure is 120 μm high and the diameter of the chamber is 6 mm. The fabrication processes of the SU-8 micro-structure are shown in Fig. 4 and described as follows. (1) The wafer was cleaned by a chemical reagent (H_2SO_4 : H_2O_2=3 : 1) and then dehydrated at 90 ^{0}C for 10 minutes as shown in Fig. 4(a). (2) A thin layer of SU8-50 photoresist with 120 μm thickness as shown in Fig. 4(b) was spin-coated on the wafer. (3) The photoresist was partially evaporated on a hot plate by two stages, as shown in Fig. 4(c). The first one was pre-baked at 65 ^{0}C for 15 minutes, and the second stage was soft baked at 95 ^{0}C for 50 minutes. After that, it was slowly cooled to room temperature. (4) The photoresist was exposed by the UV photolithography as shown in Fig. 4(d) with near 365 nm wave length such that this negative resist was polymerized. (5) A post exposure baking (PEB) was executed on a hot plate by two stages, as shown in Fig. 4(e). The first stage was at 65 ^{0}C for 5 minutes, and the second stage was at 95 ^{0}C for 15 minutes. After that, it was slowly cooled to room temperature. (6) The micro-structure was developed for 15~30 minutes by TMAH (Tetramethylammonium Hydroxide) developer, as shown in Fig. 4(f). (7) After that, the structure was rinsed by deionized water as well as dried by nitrogen as shown in Fig. 4(g) and put in an oven with 120 ^{0}C for 120 minutes as shown in Fig. 4(h). Then it was slowly cooled to room temperature. One example of the fabricated nozzle/diffuser is shown in Fig. 5.

The cover was fabricated from polydimethylesiloxane (PDMS) material because it is easy to bond with the micro-structure. This cover was a square with 20 mm x 20 mm. A mold of SU-8 photoresist, which was used to cast the PDMS, was fabricated by employing UV exposure and film mask. After mixing Sylgard 184 A and B with the volume ratio of 10 to 1, the PDMS was filled into the SU-8 mold, and the mold was kept still for 30 minutes in order to have a smooth surface. Then, it was put in a vacuum oven with

120 ^{0}C for 2 hours such that the bubbles in the PDMS were sucked out.

After finishing the four components, the micropump was assembled by the following processes. (1) The PDMS was composed of Sylgard 184 A and B with the volume ratio of 10 to 1, and it was put at rest for 4~5 hours. (2) The copper plate of the piezoelectric buzzer was laid with a small amount of PDMS that was a nonconductor. (3) The edge of the micro-structure was also spread with a small amount of PDMS and it was heated to 120 ^{0}C for 10 minutes. Then, the piezoelectric buzzer was bonded on the micro-structure. (4) The paste for Ag was used to bond a copper wire on the copper plate of the piezoelectric buzzer that functions as a cathode. (5) The bonding between the piezoelectric buzzer and the micro-structure was strengthened by heating to 120 ^{0}C for 30 minutes. (6) Under the assistance of a mechanical alignment system, the PDMS lid was bonded with the structure of the micropump by PDMS and then was heated to 120 ^{0}C for 1 hour. (7) A cooper wire was bonded by the paste for Ag on the ceramic of the piezoelectric buzzer that is an anode. (8) Needles of 1.1 mm outer diameter were glued in the inlet/outlet holes to assist the connection with pipes. One example of the assembled micropump is shown in Fig. 6.

To measure the volume flow rate of the assembled micropump, the experiment setup was composed of power supply, function generator, inlet, outlet, and laser displacement meter (Keyence LC-2400) as shown in Fig. 7. A tank was used in the inlet to store the tested liquid, and there was a long pipe in the outlet. The tested liquid was deionized water. Before the test, the water needed to fill the chamber. A sine wave of 60 peak-to-peak Volt was used to drive the buzzer. Owing to the extension/contraction along the in-plane direction, the buzzer would buckle up and down, and a sine oscillatory form was observed. To measure the flow rate without backpressure, the water level of the inlet was the same with that of the outlet. Then the flow rate was calculated from the distance travelled by the water in the pipe of the outlet in a certain period of time. To clearly watch the distance, red ink may be put in the water. The inner diameter of the pipe used was 1.1 mm.

4. Results and discussion

After the micropump has been assembled and deionized water has been filled, a sine wave of 60 peak-to-peak Volt is used to drive the buzzer, and the considered driving frequency is from 10 Hz to 300 Hz. The deflection occurring at the central point of the piezoelectric buzzer is measured by a laser displacement meter and shown in Fig. 8. As shown, the central deflection is approximate to be linearly decreased with respect to the increase of the driving frequency. The maximum value is about 22 μm at 10 Hz and the minimum value has about 4 μm at 300 Hz. The decrease of the central deflection could be considered to be dramatic during this short range of frequency. Generally speaking, the frequency considered here is rather low, but the actuation amplitude provided by the piezoelectric buzzer is significantly high. Therefore, one may say that the piezoelectric buzzer is an excellent actuator under low frequencies.

Under the same range of driving frequency, the volume flow rates of the thirteen micropumps are measured. These results are also shown in Figs. 9-13 according to the slenderness (L/W_1). For all these micropumps, the maximum volume flow rate always occurs at the frequency of 200 Hz. This could be contributed from the product values of the driving frequency and the deflection of the buzzer. For example, if one calculate the products of the driving frequency and the central deflection as shown in Fig. 8. The maximum product occurs at the frequency of 200 Hz. As shown in Fig. 9, the divergence angles considered are 4^0 and 20^0 for L/W_1=5. It is clear that the micropump with $2\theta=20^0$ has better volume flow rate than that with $2\theta=4^0$ over all the considered frequencies. However, their maximum flow rates are just around 55 μl/min and relatively low as compared to those of other micropumps. The volume flow rates of the micropump with L/W_1=10 are shown in Fig. 10. This figure indicates that the micropumps with $2\theta=20^0$ and $2\theta=40^0$ have very close results and are significantly higher than those with $2\theta=4^0$. For L/W_1=15, the volume flow rates of the micropump with $2\theta=10^0$ are very close to those of the micropump with $2\theta=30^0$ as shown in Fig. 11. Figure 12 shows that the difference between the three micropumps is not big, even though that with $2\theta=4^0$ has lower volume flow rate. For L/W_1=25, the three micropumps have different trend as shown in Fig. 13 with those with different values of L/W_1. When the frequency is low as from 10 to 30 Hz, the micropump with $2\theta=40^0$ has the highest volume flow rate, and that with $2\theta=10^0$ has the lowest flow rate. However, when the frequency is higher than 100 Hz, the situation is reverse.

If the maximum volume flow rates of these thirteen micropumps occurring at 200 Hz are focused and compared, the results are illustrated in Fig. 14 and Fig. 3, in which the maximum values are shown along with the diffuser number. As shown in Fig. 14, when L/W_1=5, the maximum volume flow rates of these two micropumps that are number 5 and 10 as shown in Fig. 3 are very low. Also, when $2\theta=4^0$ as shown in Fig. 14, the results are not good. These three micropumps are located in the “no stall” region as shown in Fig. 3. Similarly, as $2\theta=40^0$ that are in the “bistable steady stall” region, the volume flow rates are not good. From both figures, the better nozzle/diffuser is located in the transitory steady stall region, around L/W_1=10~25 and $2\theta=10^0$~30^0, where the flow is strongly unsteady. If a small region of these two parameters is desired, that with L/W_1=20~25 and $2\theta=10^0$~20^0 is probably a good

choice. Among them, the best two nozzles/diffusers that are numbers 4 and 13 as shown in Fig. 3 occur at the line of the maximum pressure recovery, and their maximum volume flow rates are 116 μl/min and 105 μl/min, respectively. Therefore, the nozzle/diffuser along the maximum pressure recovery should be recommended, especially, around the region of L/W_1=20~25 and $2\theta=10^0$~20^0.

5. Conclusions

Thirteen micropumps with different design of nozzle/diffuser are chosen from the no stall region, transitory region, and bistable steady stall region in a complete stability map of diffuser flow patterns. They are fabricated by UV photolithography and actuated by a piezoelectrical buzzer. To judge their performance, the volume flow rates are measured under the driving frequency from 10 to 300 Hz. The results indicate that the best driving frequency is at 200 Hz for all micropumps. This may be due to that this frequency has the highest product of the driving frequency and the deflection of the buzzer. Among these thirteen micropumps, those having better performance are located in the transitory region where the flow is strongly unsteady. If a small region of the two design parameters is desired, a good choice is probably that the slenderness is from 20 to 25 and the open angle is from 10^0 to 20^0. The best two nozzles/diffusers occur at the line of the maximum pressure recovery.

7. References

1. H. T. G. van Lintel, F. C. M. van de Pol, S. Bouwstra, A Piezoelectric Micropump Based on Micromachining of Silicon, Sens. Actuators A, Vol. 15, pp. 153-167, 1988.
2. E. Stemme, G. Stemme, A Valve-less Diffuser/nozzle-based Fluid Pump, Sens. Actuators A, Vol. 39, pp. 159-167, 1993.
3. A. Olsson, G. Stemme, E. Stemme, Diffuser-element Design Investigation for Valve-less Pumps, Sens. Actuators A, Vol. 57, pp. 137-143, 1996.
4. A. Olsson, G. Stemme, E. Stemme, Numerical and Experimental Studies of Flat-walled Diffuser Elements for Valve-less Micropumps, Sens. Actuators A, Vol. 87, pp. 165-175, 2000.
5. K. S. Yang, , I. Y. Chen, B. Y. Shew, C. C. Wang, Investigation on the Flow Characteristics within a Micronozzle/diffuser, J. Micromech. Microengineering, Vol. 13, pp. 1-6, 2003.
6. V. Singhal, S. V. Garimella, J. Y. Murthy, Low Reynolds Number Flow through Nozzle-diffuser Elements in Valveless Micropumps, Sens. Actuators A, Vol. 113, pp. 226-235, 2004.
7. Q. Yao, D. Xu, L. S. Pan, A. L. Melissa Teo, W. M. Ho, V. S. Peter Lee, M. Shabbir, CFD Simulations of Flows in Valveless Micropumps, Eng. Appl. Comput. Fluid Mech., Vol. 1, pp. 181-188, 2007.
8. I. Izzo, D. Accoto, A. Menciassi, L. Schmitt, P. Dario, Modeling and Experimental Validation of a Piezoelectric Micropump with Novel No-moving-part Valves, Sens. Actuators A, Vol. 133, pp. 128-140, 2007.
9. Y. C. Wang, J. C. Hsu, P. C. Kuo, Y. C. Lee, Loss Characteristics and Flow Rectification Property of Diffuser Valves for Micropump Applications, Int. J. Heat Mass Transf., Vol. 52, pp. 328-336, 2009.
10. Y. T. Chen, S. W. Kang, L. C. Wu, S. H. Lee, Fabrication and Investigation of PDMS Micro-diffuser/nozzle, J. Mater. Process. Technol., Vol. 198, pp. 478-484, 2008.
11. F. M. White, Fluid Mechanics, McGraw-Hill, New York, 1979.

8. Chart arrangement

Table 1 Dimensions of diffusers

Diffuser	L(μm)	W_2(μm)	2θ(degree)	L/W_1
1	1200	994	40	10
2	1800	1085	30	15
3	2400	967	20	20
4	3000	645	10	25
5	600	162	4	5
6	1200	204	4	10
7	2400	288	4	20
8	3000	1178	20	25
9	3000	2304	40	25
10	600	332	20	5
11	1200	544	20	10
12	1800	335	10	15
13	2400	540	10	20

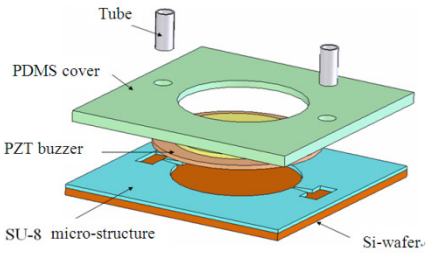

Fig. 1 Parts of a valveless micropump

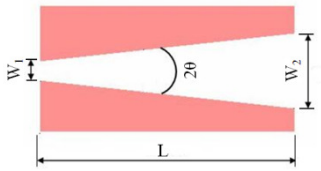

Fig. 2 Dimensions of a nozzle/diffuser

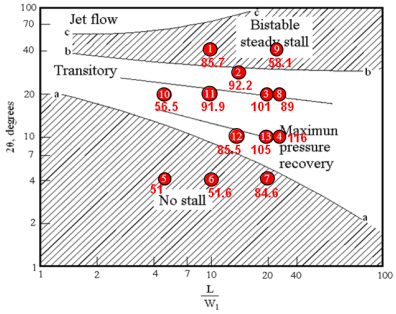

Fig. 3Thirteen designs in a complete stability map of diffuser flow patterns

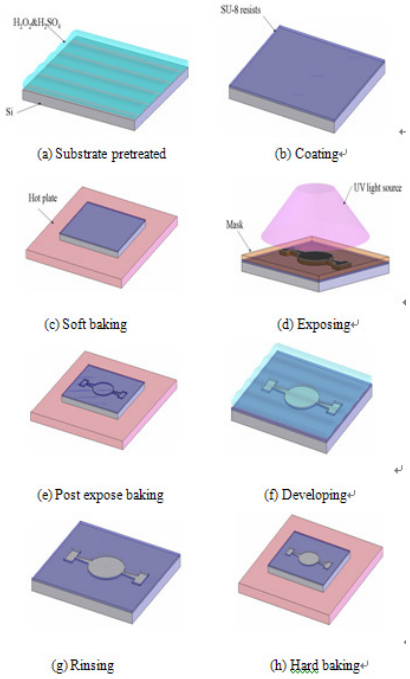

Fig. 4 Fabrication processes of SU-8 micro-structure

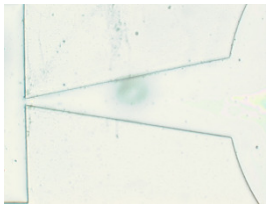

Fig. 5 One example of the fabricated nozzle/diffuser

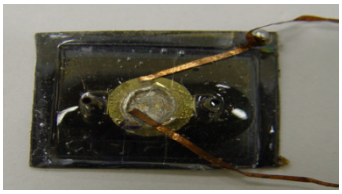

Fig. 6 One example of the assembled micro pump

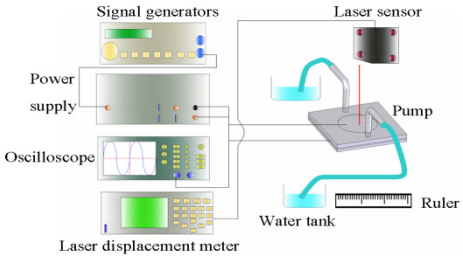

Fig. 7 Experiment setup for measuring volume flow rate

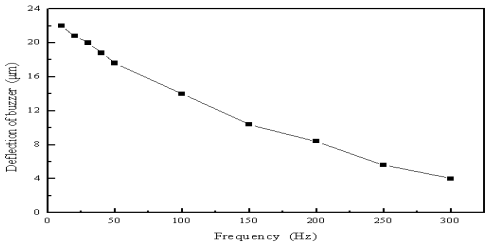

Fig. 8 Maximum deflection of buzzer under different frequencies

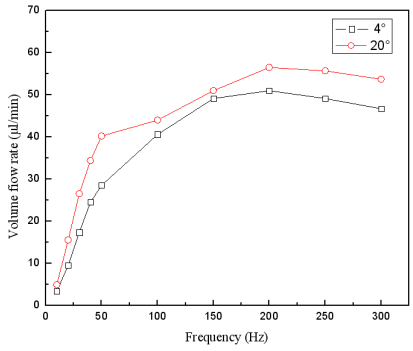

Fig. 9 Volume flow rate of micropumps with slenderness $L/W_1=5$

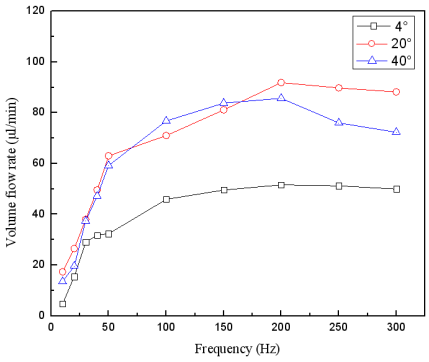

Fig. 10 Volume flow rate of micropumps with slenderness L/W_1=10

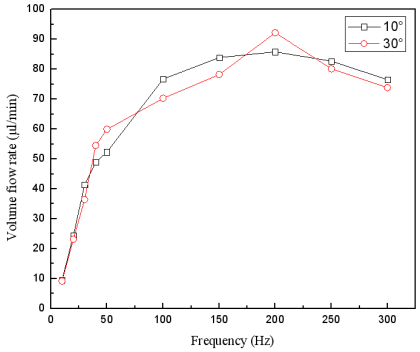

Fig. 11 Volume flow rate of micropumps with slenderness L/W_1=15

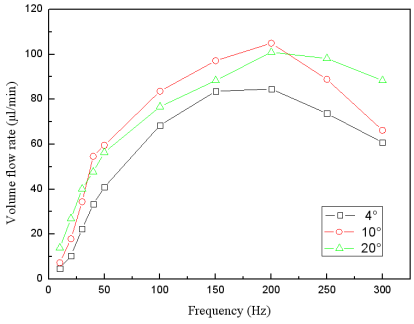

Fig. 12 Volume flow rate of micropumps with slenderness L/W_1=20

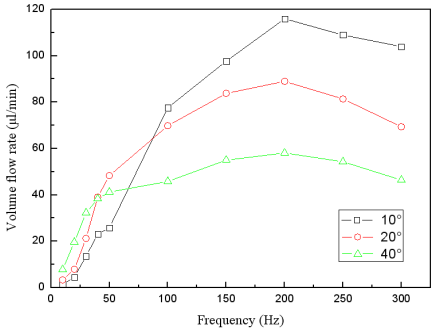

Fig. 13 Volume flow rate of micropumps with slenderness L/W_1=25

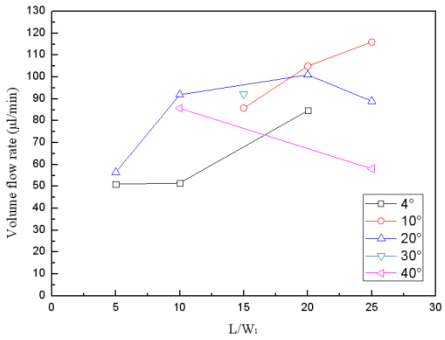

Fig 14 Volume flow rate with respect to slenderness L/W_1 and divergence angle 2θ

無閥式微幫浦噴嘴/擴散口最佳設計的實驗探討

黃順發[1]、紀穎旻[1]
[1]國立雲林科技大學機械工程系

摘要

為了設計平面型噴嘴/擴散口，它的兩個參數，擴散角及細長比，將利用實驗量測整個微幫浦的體流率來探討。13 組微幫浦選自於擴散器穩定圖的非失速區、短暫區、雙穩定區。這些微幫浦將利用壓電蜂鳴片來趨動並利用微影製程來製造。量測結果顯示來自於短暫區的微幫浦有較佳的體積流率。最佳的兩組微幫浦是落在最大壓力恢復線上。

關鍵字：微幫浦、噴嘴/擴散口、壓電蜂鳴片、擴散角、細長比